

ESTIMATION OF BURN INJURIES FROM TEMPERATURE MEASUREMENT USED IN EVALUATION OF FIRE PROTECTIVE GARMENTS

Matej Gašperin, Dani Juričič, Bojan Musizza, Igor Mekjavič

Jožef Stefan Institute
1000 Ljubljana, Jamova 39, Slovenia
matej.gasperin@ijs.si (Matej Gašperin)

Abstract

The overall performance of thermal protective clothing can be evaluated either by means of bench scale test or by exposing a dressed mannequin to real-life flame conditions. In this paper an automated system for evaluation of fire protective clothing based on the use of a flame mannequin is presented. The mannequin is equipped with an array of temperature sensors which provide the information about the temperature on the mannequin surface. The level of burn injury is evaluated using the estimated heat flux entering the material at the surface and thermal skin model. A particular attention in this paper is focused on the issue of heat flux reconstruction, with special focus on the computational demands of the algorithms. Two appropriate algorithms for heat flux reconstruction are presented and evaluated on calibration measurement. The estimated heat flux is later used in the skin thermal model which calculates the temperature profiles inside the skin. The process of skin burn evolution is represented as a first order chemical reaction at two points inside the skin profile. The degree of burn is determined using well established empirical rules. A special attention is again given to the issue of computational load of the solution resulting in an efficient algorithm for calculation of skin temperature profile. The effectiveness of the solution is demonstrated on experimental data and an example of experimental run is provided.

Keywords: Modeling, inverse heat conduction problem, Burn prediction, Parameter estimation, Mannequin test

Presenting Author's Biography

Matej Gašperin got his BSc degree from the Faculty of Electrical Engineering, University of Ljubljana in 2006. He is now a PhD student at Jožef Stefan International Postgraduate School and working at the Jožef Stefan Institute, Department of Systems and Control as a junior researcher. His current research areas are Simulation and modeling of thermal processes and environmental ergonomics.



1 Introduction

Workers in many industrial settings, firefighters and soldiers are likely to be exposed to excessive heat caused by flash fire. Analysis of numerous accidents reveals, that the heat fluxes can be relatively high (up to $80\text{kW}/\text{m}^2$), but the exposure only lasts about 2 – 10 seconds. [8]. The role of protective clothing is to minimize or prevent skin burn injuries by decreasing the heat transfer from the fire to the skin. In order for the manufacturers to fabricate suitable wear it is essential that the protective characteristics of the garments can be evaluated.

Quantitative evaluation of thermal protective garments to fire exposure can be performed either by means of bench scale test [17] or by exposing a dressed mannequin to real-life flame conditions. However bench scale tests can not provide complete information because the effects like zippers, layers of outfit, etc. can not be properly taken into account. Much more faithful insight can be obtained if the experiment is made as realistic as possible by using instrumented flame mannequins.

In this paper an automated system for testing the garments under flash fire is presented. The system is build around a flame mannequin equipped with 144 temperature sensors, which provide information about temperature on the mannequin surface. The system is realized in conformance with the standards for carrying out garment assessment [11]. The project is motivated by rising need of the manufacturers of protective garments for additional assessment facilities, since more independent tests carried out at different laboratories contribute to more objective evaluation of a particular garments [4]. The main focus of the paper is to carefully revisit the issue of heat flux reconstruction from temperature readings with the aim to provide the computational procedure that will support all operating regimes of the sensor. The paper will also review the process of estimation of burn injuries using a detailed skin model and suggest a computationally efficient algorithm for its calculation.

2 System architecture

The main building blocks of the systems are shown in Fig. 1. The core of the system represents a flame mannequin located in a firing room. A flash fire reproduction system consists of 12 gas burners mounted around the mannequin. The signals from thermocouples on the mannequin are collected by data acquisition system running under LabVIEW environment. To ensure a higher safety, the operation is governed by a programmable logic controller rather than LabVIEW directly. The application allows the operator to control all stages of the experiment and automatically generates detailed reports on the experiment.

Due to safety and calibration issues, the experiment procedure is strictly determined. Prior to the start of the experiment a 30 second venting of the room is performed to ensure the room is filled with clean air. Next,

safe and pilot burners are switched on in order to ensure the burners and gas supply are in fault free condition. After that a calibration procedure is performed in which a nude mannequin is subjected to 3 – 4 second flash fire. For each sensor a corresponding heat flux is calculated. Based on that heat flux, the burners are adjusted to ensure an average heat flux around $80\text{kW}/\text{m}^2$. Now the system is ready for the garment evaluation. The mannequin is dressed and exposed to flash fire for 2 – 10 seconds. After the fire extinguishes another venting of the room is performed and the facility is ready for next experiment.

The quality of the garment is assessed with respect to the percentage of the skin area affected by first, second or third degree burns. The procedure for estimation of the burn degree consists of three major steps:

1. from the recorded temperature on the mannequin surface heat flux is calculated
2. temperatures inside the skin are calculated using thermal model of the skin and estimated heat flux
3. using these temperatures the degree of burn is calculated using burn integral.

3 Inverse heat conduction problem

The critical part of the burn injury level estimation is the calculation of the heat flux entering the material from measured temperature at the surface of the material. In this paper algorithms for heat flux reconstruction using temperature gradient at the material surface have been examined. First a detailed thermal model of the sensor described with partial differential equation has been used. The heat conduction across the sensor has been solved using a finite differences and Crank-Nicolson scheme [20]. The algorithm, referred to as CN scheme is than compared to the simplified sensor model using one ordinary differential equation with lumped parameters (ODE).

One other issue to be resolved are the material thermal parameter values used in the models. The unknown parameter values have been estimated using optimization procedure and mannequin sensor readings. For this purpose, a calibration procedure has been conducted, so that the temperature and heat flux sensor have been exposed to the same heat source. The experiment has been repeated 33 times, using the same duration of the flame (5 seconds). The resulting dataset will serve for validation of the algorithms. One additional measurement data have been obtained and will be used as a training dataset for parameter estimation.

3.1 Distributed parameters sensor model

As mentioned above, one approach of determining heat flux is by using temperature gradient. The temperature sensor is cylindrical slab, cca. 3cm long with thermocouple mounted inside. Heat transfer across the sensor can be described with the following model:

$$\frac{\partial u}{\partial t} = \alpha \frac{\partial^2 u}{\partial x^2} \quad (1)$$

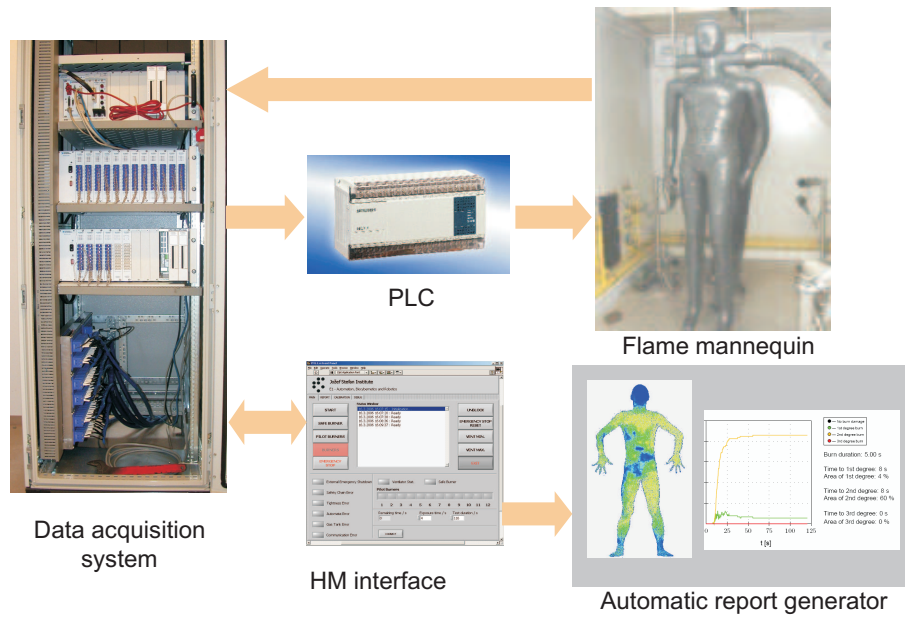


Fig. 1 Architecture of the instrumented mannequin system

$$\begin{aligned}
 t = 0, x \geq 0, T(t = 0, x) &= T_0 \\
 t > 0, x = 0, T(t, 0) &= T_M(t) \\
 t > 0, x = l, -k \frac{\partial T}{\partial x} &= -\lambda(T(l, t) - T_0)
 \end{aligned}$$

The model has been formulated in this way, because the sensor has a finite depth and due to low thermal resistance the cooling on the lower edge of the sensor has to be properly taken into account.

The numerical solution of the expression (1) is obtained by substituting the continuous partial derivatives with finite differences. First order time derivative is approximated with forward difference (2) and second order space derivative with central difference (3). Index i stands for i -th point in the x axis grid and index j for j -th time sample. Δt is discrete time step or in our case also sampling time which is 0.06s, Δx is the discrete space step which has a value of 0.01.

$$\frac{\partial T}{\partial t} = \frac{T_{j+1,i} - T_{j,i}}{\Delta t} \quad (2)$$

$$\frac{\partial^2 T}{\partial x^2} = \frac{T_{j,i-1} - 2T_{j,i} + T_{j,i+1}}{\Delta x^2} \quad (3)$$

By reformulating the equation and substituting $\alpha \frac{\Delta t}{(\Delta x)^2}$ with Λ , system of the following expressions is produced:

$$\begin{aligned}
 -\Lambda T_{i-1,j+1} + 2(1 + \Lambda)T_{i,j+1} - \Lambda T_{j+1,i+1} &= \\
 = \Lambda T_{j-1,i} + 2(1 - \Lambda)T_{j,i} + \Lambda T_{j+1,i} & \quad (4)
 \end{aligned}$$

Adding the two boundary condition at $x = 0$ and $x = l$ in difference form:

$$T_{0,j} = T_{su,j} \quad (5)$$

$$\left(1 - \frac{\lambda \Delta x}{k}\right) T_{M,j} - T_{M-1,j} = -\frac{\lambda \Delta x}{k} T_0 \quad (6)$$

where M is the number of the points in x axis grid, T_{su} is measured temperature and T_0 is the environment temperature. The expressions (4), (5) and (6) form a tri-diagonal system of equations. The temperature at all data points in the next time step ($j + 1$) is expressed in matrix form and is calculated with LU-decomposition. In the matrix form it reads

$$\mathbf{A}_1 \mathbf{T}_j = \mathbf{A}_0 \mathbf{T}_{j-1} + \mathbf{c}_{j-1} \quad (7)$$

The temperature distribution within the body is obtained by iterative calculation of (7), which results in the temperature profile $\{T_{i,j}, i = 1, 2, \dots, M\}$. Then it is easy to find the heat flux at time t_j

$$q_j = -k \frac{T_{1,j} - T_{0,j}}{\Delta x} \quad (8)$$

Next step represents the estimation of the material thermal parameters from calibration data. The calibration set-up is illustrated in Figure 2. A flux sensor and a temperature sensor, mounted on a panel, are exposed to the common heat source. The unknown parameter is then found by optimization of the criterion function:

$$J_{CN}(\boldsymbol{\theta}_1) = \frac{\int_0^\tau (q(t) - q_M(t))^2 dt}{\int_0^\tau q_M(t)^2 dt} \quad (9)$$

where $\boldsymbol{\theta}_1$ represents the vector of unknown model parameters $[\lambda, \rho c, k]$, $q(t)$ is estimated heat flux and $q_M(t)$

is measured heat flux. The minimum of the criterion function $J(\theta_1)$ is found using constrained linear optimization in MATLAB using Nelder-Mead method. The use of constrains is necessary in order to prevent negative values of the parameters.

$$\{\lambda^*, \rho c^*, k^*\} = \operatorname{argmin}_{\lambda \in [0, \infty], \rho c L \in [0, \infty]} J(\theta_1) \quad (10)$$

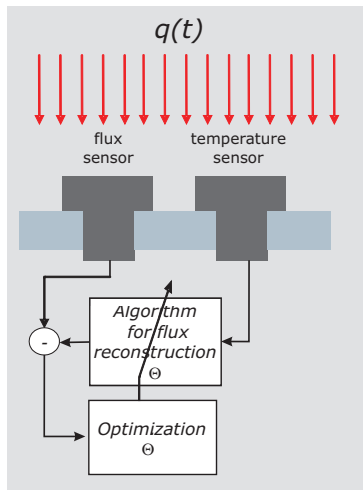


Fig. 2 The calibration setup (θ represents vector of unknown parameters)

Using the estimated parameter values the heat flux estimate shown in Fig. 3 is obtained.

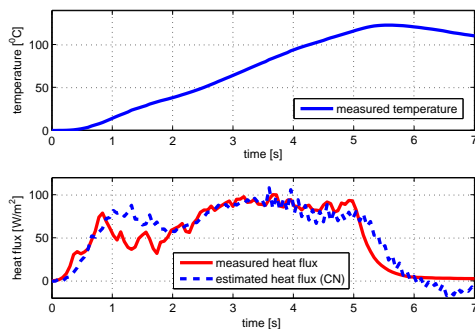


Fig. 3 Measured and reconstructed heat flux by means of Crank-Nicolson method

The algorithm describes the exact situation within the sensor, but its drawback is, that the recursion (7) has to be calculated for all the temperature sensors which represents a computationally demanding procedure. Fortunately there exist a much shorter way to obtain the heat flux entering the material $q(t)$.

Using the relation $c_j = [\Lambda, 0, \dots, 0]^T T_{su,j} = c T_{su,j}$, where $T_{su,j}$ is the measured surface temperature, the expressions for the temperature profiles at times $j = 1, 2, \dots, N$ are of the following form

$$\begin{aligned} \mathbf{T}_1 &= \mathbf{A}_1^{-1} \mathbf{A}_0 \mathbf{T}_0 + \mathbf{A}_1^{-1} \mathbf{c}_0 = \mathbf{A}_1^{-1} \mathbf{c}_0 \\ \mathbf{T}_2 &= \mathbf{A}_1^{-1} \mathbf{A}_0 \mathbf{T}_1 + \mathbf{A}_1^{-1} \mathbf{c}_1 \\ &= \mathbf{A}_1^{-1} \mathbf{A}_0 \mathbf{A}_1^{-1} \mathbf{c}_0 + \mathbf{A}_1^{-1} \mathbf{c}_1 \\ &\vdots \\ \mathbf{T}_N &= (\mathbf{A}_1^{-1} \mathbf{A}_0)^{N-1} \mathbf{A}_1^{-1} \mathbf{c}_{N-1} + \\ &+ (\mathbf{A}_1^{-1} \mathbf{A}_0)^{N-2} \mathbf{A}_1^{-1} \mathbf{c}_{N-2} + \dots + \\ &+ \mathbf{A}_1^{-1} \mathbf{c}_0 \end{aligned} \quad (11)$$

The coefficients in the expressions (11) represent the elements of the system impulse response and can all be written in form of one matrix expression

$$\mathbf{q} = \mathbf{\Gamma} \mathbf{T}_{su} \quad (12)$$

where \mathbf{q} represents the estimated heat flux, $\mathbf{\Gamma}$ is the lower triangular matrix, with rows representing system impulse response and \mathbf{T}_{su} is the vector containing surface temperature readings. The elements of the impulse response (matrix $\mathbf{\Gamma}$) can all be calculated prior to the experiment and thus the time needed for calculation of the results is greatly shortened.

3.2 Lumped parameter sensor model

Due to the relatively high thermal conductivity with respect to sensor depth, the heat transfer along the sensor can be approximated with lumped parameter model. Here it is assumed, that the temperature of the body is the same at all depths and the change of the temperature is proportional to the heat fluxes entering and exiting the material. The temperature change of the material as a result of heat flux can be expressed as $\rho v c \frac{dT}{dt}$. Heat flux entering the material depends on the area being exposed to it ($Aq(t)$), heat flux at the other end of the material depends on the heat transfer coefficient and surrounding temperature ($\lambda(T(t) - T_0(t))$). The sum of all heat fluxes and accumulated heat equals 0 (13).

$$\rho V c \frac{dT}{dt} - Aq(t) + \lambda(T(t) - T_0(t)) = 0 \quad (13)$$

Expressing $q(t)$ from Eq. (13):

$$q(t) = \frac{dT(t)}{dt} (\rho c L) + \lambda(T(t) - T_0) \quad (14)$$

The continuous derivative in Eq. (14) is calculated numerically using finite differences with backward scheme.

$$\left. \frac{dT(t)}{dt} \right|_{t=t_j} = \frac{T_j - T_{j-1}}{\Delta t} \quad (15)$$

To estimate the heat flux $q(t)$ from expression (14), there are two unknown parameter values ($\lambda, \rho c L$). The

values are estimated similar to the ones described in previous section, with optimization of the heat flux estimate using the criterion function Eq. (16).

$$J_{CN}(\theta_2) = \frac{\int_0^\tau (q(t) - q_M(t))^2 dt}{\int_0^\tau q_M(t)^2 dt}, \quad (16)$$

where θ_2 is vector of unknown parameters $[\lambda, \rho c l]$, $q(t)$ estimated heat flux and $q_m(t)$ measured heat flux. The minimum of the criterion function $J(\theta_2)$ is again found using constrained linear optimization to prevent negative values of the parameters.

$$\{\lambda^*, \rho c l^*\} = \operatorname{argmin}_{\lambda \in [0, \infty], \rho c l \in [0, \infty]} J(\theta_2) \quad (17)$$

Using the training dataset we obtain the estimated heat flux as shown in Fig. (4).

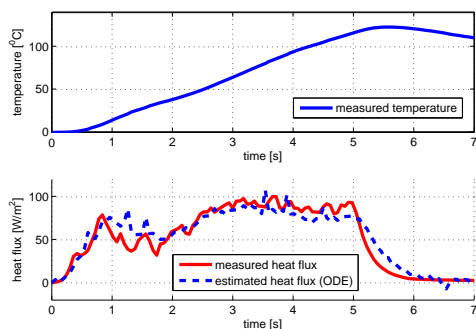


Fig. 4 Comparison between measured and estimated heat flux using training dataset

3.3 Algorithm comparison

The quality of the reconstructed heat fluxes using the two algorithms described above has been evaluated on the test datasets consisting of 33 measurement from calibration procedures performed under the same conditions as the training dataset. The criterion function values (16) and (9) have been calculated for every member of the test dataset and for both algorithms. The resulting criterion function value probability distributions are shown in Fig. 5.

Comparing the results (Fig. 5), one can see that with using the ODE based algorithm criterion function value probability distribution is in fact lower than the one obtained using Crank-Nicolson scheme. Therefore the later approach is not only significantly less computationally demanding, but also offers better quality of the estimate. The results suggests that the CN scheme parameters may be overfitted and therefore the solution is not the most appropriate for different operating regimes.

4 Estimation of burn injuries

The next step in the calculation of burn injuries is the calculation of the temperature profile in the skin. For

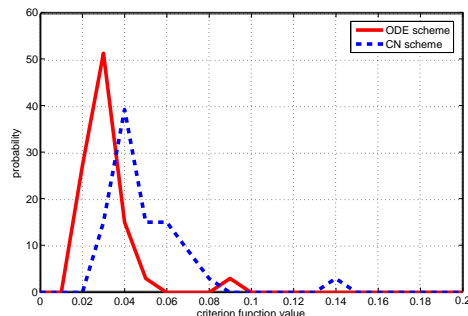


Fig. 5 Criterion function value probability distributions

the purpose of this paper, the skin can be viewed as composed of three layers:

- *epidermis*, thin outer layer of typical thickness $0.06 - 0.8\text{mm}$
- *dermis*, $1 - 4\text{mm}$ thick directly below the epidermis; provides the strength and elasticity for the skin, and contains lymphatic vessels, nerves, and blood vessels.
- *subcutaneous tissue* ($1.5 - 2\text{cm}$ thick), connective tissue serving for formation and storage of fat.

The skin response to thermal insult has been treated by a number of studies in the last 50 years. Henriques [10] and later Mehta [14] have found that injury starts to evolve when temperature becomes greater than 317K . The proposed burn injury evaluation models rely on the idea of Henriques [10], according to which the process can be viewed as a first-order chemical reaction

$$\frac{d\Omega}{dt} = \begin{cases} 0 & T < 317\text{K} \\ P e^{-\frac{\Delta E}{RT}} & T \geq 317\text{K} \end{cases} \quad (18)$$

where Ω is burn integral, P is a factor, $\frac{\Delta E}{R}$ activation energy, T absolute temperature of the tissue. However, the models explaining the emergence of injury differ somewhat and the coefficients used have different values (c.f. Table 1). In our studies we follow the recommendations [5], [11], [1] to combine the Stoll's burn criteria at depth $x_d = 0.08\text{mm}$ (epidermis-dermis boundary) and Takata's criteria at depth $x_s = 0.2\text{cm}$ (boundary between dermis and subcutaneous region). The values of the parameters are given in Table 1. The degree of burn is determined according to the empirical rules stressed in Table 2.

Essential for the calculation of the burn rate (18) is determination of the temperatures at the interface between epidermal and dermal layer (x_1) and dermal and subcutaneous region (x_2). The calculation procedure is illustrated in Fig. 6. Since the mannequin is instrumented with temperature sensors, first the corresponding flow of heat flux has to be estimated. Based on that, the temperature profile along the skin layers as function of time is calculated.

Tab. 1 Coefficients of Stoll's and Takata's model

	Stoll	Takata
$T < 50^\circ C$	$P = 2.185 \times 10^{124} s^{-1}$ $\frac{\Delta E}{R} = 93535K$	$P = 4.32 \times 10^{64} s^{-1}$ $\frac{\Delta E}{R} = 50000K$
$T \geq 50^\circ C$	$P = 1.823 \times 10^{51} s^{-1}$ $\frac{\Delta E}{R} = 39110K$	$P = 9.39 \times 10^{104} s^{-1}$ $\frac{\Delta E}{R} = 80000K$

Tab. 2 Categories of burn injuries and corresponding computational rules

$\Omega \leq 0.5$ at x_d	No burn injury
$0.5 < \Omega < 1$ at x_d	First degree injury
$1 \leq \Omega$ at x_d AND $\Omega < 1$ at x_s	Second degree injury
$0.5 \leq \Omega$ at x_s	Third degree injury

It is assumed that heat transfer in the skin can be described by the following partial differential equation (PDE) [5]

$$\rho c \frac{\partial T}{\partial t} = k \frac{\partial^2 T}{\partial x^2} - G(\rho c)_b(T - T_0) \quad (19)$$

where T denotes temperature, x depth, c specific heat, G blood perfusion rate, k thermal conductivity and index $(\rho c)_b$ indicates the volumetric heat capacity of blood, T_0 is blood perfusion temperature, where the values for each skin layer are known [15, 1]

The following initial and boundary conditions are applied

$$T(x, t = 0) = T_0, \quad 0 \leq x \leq D \quad (20)$$

$$k \frac{\partial T}{\partial x} \Big|_{x=0} + q(t) = 0 \quad (21)$$

$$T(x = D, t) = T_0 \quad (22)$$

where D is skin thickness and $q(t)$ heat flux (the same as sensed by the mannequin surface). At the interface between two different layers (at $x = x_d$ and $x = x_s$) the equality of heat fluxes hold, i.e.

$$k_1 \frac{\partial T}{\partial x} \Big|_{x_d^-} = k_2 \frac{\partial T}{\partial x} \Big|_{x_d^+}$$

$$k_2 \frac{\partial T}{\partial x} \Big|_{x_s^-} = k_3 \frac{\partial T}{\partial x} \Big|_{x_s^+}$$

with k_1 , k_2 and k_3 being thermal conductivity of epidermal, dermal and subcutaneous layer respectively.

The numerical solution of expression (19) is obtained by substituting the continuous partial derivatives with finite differences. Crank-Nicolson method has been used, which can be interpreted as an average between fully explicit and fully implicit method. One-dimensional grid is spanned over the skin profile so that

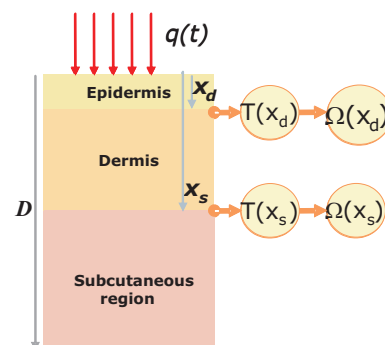


Fig. 6 The principle of estimation of burn injury

the distance between discretization points within a particular layer is constant. Thus reasonable accuracy is achieved if 20, 40 and 100 intervals are used for epidermal, dermal and subcutaneous layer respectively.

Calculation of the temperature profile at time $j\Delta t$ $\mathbf{T}(j) = [T_{0,j}, T_{1,j}, \dots, T_{N,j}]^T$ along the discrete points of one-dimensional mesh $\{x_0, x_1, \dots, x_N\}$ is performed in recursive manner by solving the following equation by means of LU-decomposition.

$$\Psi_1 \mathbf{T}_j = \Psi_0 \mathbf{T}_{j-1} + \mathbf{b}q_j \quad (23)$$

The calculation is again computationally relatively demanding since it has to be performed for all 144 sensors. If the expressions for every time step j are written explicitly the following result is obtained

$$\begin{aligned} \mathbf{T}_1 &= \Psi_1^{-1} \Psi_0 \mathbf{T}_0 + \Psi_1^{-1} \mathbf{b}q_1 = \Psi_1^{-1} \mathbf{b}q_1 \\ \mathbf{T}_2 &= \Psi_1^{-1} \Psi_0 \mathbf{T}_1 + \Psi_1^{-1} \mathbf{b}q_2 = \\ &= \Psi_1^{-1} \Psi_0 \Psi_1^{-1} \mathbf{b}q_1 + \Psi_1^{-1} \mathbf{b}q_2 \\ &\vdots \\ \mathbf{T}_N &= (\Psi_1^{-1} \Psi_0)^{N-1} \Psi_1^{-1} \mathbf{b}q_1 + \\ &+ (\Psi_1^{-1} \Psi_0)^{N-2} \Psi_1^{-1} \mathbf{b}q_2 + \dots + \\ &+ \Psi_1^{-1} \mathbf{b}q_N \end{aligned} \quad (24)$$

It can be seen, that the coefficients in the expressions (24) represent the impulse response of the system. Using

$$\begin{aligned} T_{d,j} &= (0, \dots, 0, \underbrace{1}_{x_d}, 0, \dots, 0) \mathbf{T}_j \\ T_{s,j} &= (0, \dots, 0, \underbrace{1}_{x_s}, 0, \dots, 0) \mathbf{T}_j \end{aligned} \quad (25)$$

we can write

$$\mathbf{T}_d = \Gamma_d \mathbf{q} \quad (26)$$

$$\mathbf{T}_s = \Gamma_s \mathbf{q} \quad (27)$$

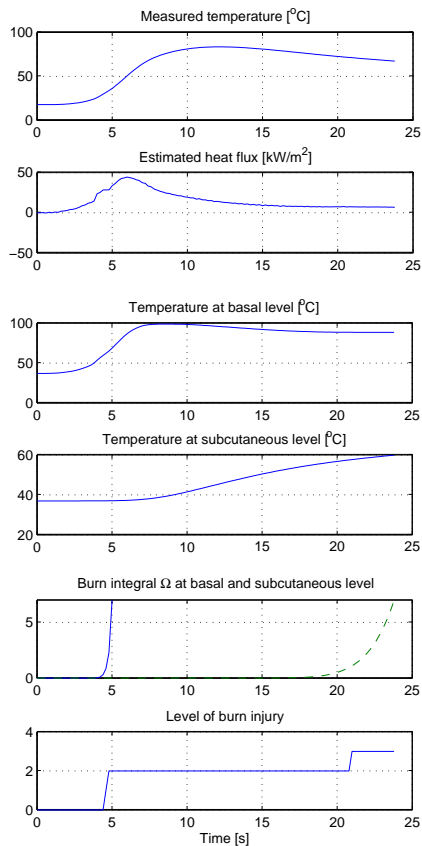


Fig. 7 Recorded temperature at a spot on the mannequin surface, reconstructed flux, simulated temperatures at basal and subcutaneous level, the evolution of burn integral and resulting injury level.

In this notation, all the elements of the lower triangular matrices Γ_b and Γ_s can be calculated off-line prior to the start of the experiment. What remains to be done on-line is only relatively simple matrix multiplication.

5 Garment assessment experiment results

In the sequel and excerpt from an assessment of a protective garment will be presented. Figure 7 shows the measured temperature, estimated heat flux, simulated temperatures inside the skin, burn integral value and finally the level of burn injury for one sensor location. This procedure is repeated for all 144 sensors and results are summarized and gathered in the report. The example of the report, namely the overall burn injury is shown in Fig. 5. The system also plots a 3D view of the distribution of injuries over the mannequin surface (Fig. 5).

6 Conclusion

The paper presents a structure of fire protective garments assessment system, with special emphasis to the heat flux reconstruction and thermal modeling of human skin.

It has been shown, that simplification of the sensor

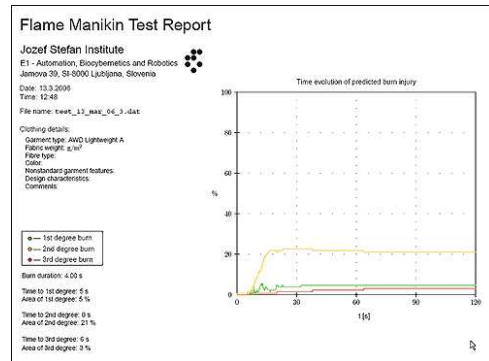


Fig. 8 Excerpt from the final report: time evolution of the burn injuries on one of the spots of the mannequin surface (green: first degree, orange: second degree, red: third degree).

offers better results in terms of heat flux reconstruction than numeric calculation of the more complex distributed parameters model. Together with the adoption of an efficient skin temperature calculation algorithm presented, the procedure for estimation of burn injury level becomes manageable in terms of computational load and also offers extremely good quality of the result (less than 5% error in heat flux reconstruction).

Future work will be focused on the influence of the variable skin properties on the burn estimates (some investigation has been already done by Torvi and Dale [17]).

Acknowledgment

The underlying work has been supported by the Slovenian Research Agency through the grant P2-0001.

7 References

- [1] ASTM, *Standard Test Method for Evaluation of Flame Resistant Clothing Protection Against Flash Fire Simulations Using an Instrumented Manikin*, 1999, The Annual Book of ASTM Standards.
- [2] Beck, J. V., Blackwell, B., St. Clair jr., C.R., *Inverse Heat conduction, Ill-posed Problems*, 1986, Wiley, New York.
- [3] Berntsson, F., *Numerical Solution of an Inverse Heat Conduction Problem*, 1998, Linköpings universitet, Sweden.
- [4] Camenzind, M.A., Dale, D.J., Rossi, R. M., *Manikin test for flame engulfment, 2007, Fire and Materials* (in press).
- [5] Crown, E.M., Dale, J.D., *Evaluation of flash fire protective clothing using an instrumented mannequin*, 1992, Report, University of Alberta.
- [6] Diller, T. E., *Methods of Determining Heat Flux From Temperature Measurement*, 1996, Proceedings of the 42nd International Instrumentation Symposium, Aerospace Industries Division and Test Measurement Division of ISA.

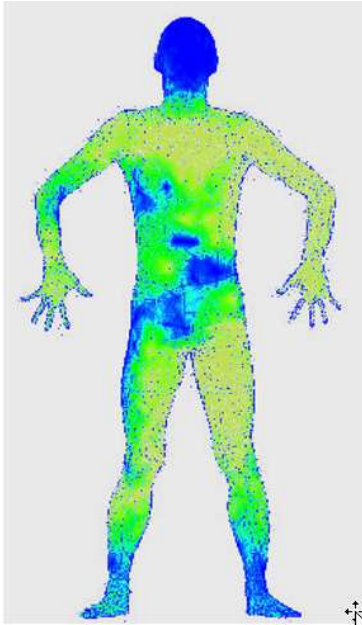


Fig. 9 3D presentation of the distribution of injury depths

- [7] Elkins, W., Thompson, J.G., *Instrumented Thermal Mannikin*, 1973, Technical Report ASD-TR-73-33, NTIS.
- [8] Gagnon, D., *Evaluation of New Test Methods for Fire Fighting Clothing*, 2000, MSc Thesis, Worchester Polytechnic Institute.
- [9] Heath, M.T., *Scientific Computing: An Introductory Survey*, McGraw-Hill, 2002, New York.
- [10] Henriques, F.C., Studies of thermal injury: The predictability and the significance of thermally induced rate process leading to irreversible epidermal injury, 1947, *Archives of Pathology*, Vol. 43, p. 489.
- [11] ISO, *Protective Clothing Against Heat and Flame - Test Method for Complete Garments - Prediction of Burn Injuries Using an Instrumented Manikin*, 2004, ISO/TC 94 ISO/DIS 13506, Geneva.
- [12] D. Juričič, M. Gašperin, B. Musizza, I. Mekjavič, M. Vrhovec, G. Dolanc, Evaluation of fire protective garments by using instrumented mannequin and model-based estimation of burn injuries, *Proceedings of the 15th Mediterranean Conference on control and Automation*, 2007
- [13] Lu, X., Tervola, P., Viljanen, M., A new analytical method to solve the heat equation for a multi-dimensional composite slab, 2005, *Journal of Physics*, A: Mathematical and General, 38 pp. 28732890.
- [14] Mehta, A.K., Wong, F., Measurement of flammability and burn potential of fabrics, 1972, Technical Report COM-73-10950, NTIS.
- [15] Staples, R., Development of a thermal manikin to test the protection offered by clothing assemblies from flame and intense heat, 1996, DCTA S&TD Research Report 96/10.
- [16] Torvi, D.A., Dale, J. D., A finite element model of skin subjected to a flash fire, 1994, *Trans. ASME*, vol. 116, pp. 250-254.
- [17] Torvi, D. A., *Heat transfer in thin fibrous materials under high heat flux conditions*, 1997, PhD Thesis, University of Alberta, Edmonton.
- [18] Walfre, F., Jie, L., Guo-Xiang, W., Nelson, J. S., Guillermo, A., Radial and temporal variations in surface heat transfer during cryogen spray cooling, 2005, *Phys. Med. Biol.*, 50 pp. 387397.
- [19] Xie, J., Zou, J., Numerical reconstruction of heat fluxes, *SIAM Journal of numerical Analysis*, 2005, vol. 43, no. 4, pp. 15041535.
- [20] Zauderer, E., *Partial Differential Equations of Applied Mathematics*, 2006, Wiley-Interscience.